



COF/MWCNTs/CLS-Based Electrochemical Sensor for Simultaneous and Sensitive Detection of Multiple Heavy Metal Ions

Jiaqi Yin¹ · Hongguo Zhai¹ · Yue Wang¹ · Bao Wang¹ · Guanglei Chu¹ · Qi Guo¹ · Yuhao Zhang¹ · Xia Sun^{1,2,3} · Yemin Guo^{1,2,3} · Yanyan Zhang^{1,2,3}

Received: 10 March 2022 / Accepted: 29 July 2022 / Published online: 3 August 2022
© The Author(s), under exclusive licence to Springer Science+Business Media, LLC, part of Springer Nature 2022

Abstract

A novel electrochemical sensor based on a covalent organic framework (COF) together with calcium lignosulfonate (CLS)-modified multiwalled carbon nanotubes (MWCNTs) and Nafion was developed for the simultaneous analysis of Cu(II), Pb(II), and Cd(II). COF with a three-dimensional (3D) porous structure containing a large number of amino groups was synthesized by the condensation of cyanuric chloride with *p*-phenylenediamine through a simple hydrothermal reaction. Therefore, COF can efficiently enrich a large number of heavy metal ions in a short time. MWCNTs significantly improved the conductivity of the sensing interface. Besides, a large number of hydrophilic groups in the structure of CLS can effectively solve the aggregation of MWCNTs. The COF nanocomposite material was characterized by transmission electron microscopy (TEM), scanning electron microscopy techniques (SEM), and Fourier-transform infrared spectroscopy (FT-IR), X-ray photoelectron spectroscopy (XPS). The influence of buffer solution type, deposition time, deposition potential, and pH in the heavy metal ion detection process were studied, and the working parameters were optimized. Under the optimal conditions, the fabricated sensor showed superior wide linear responses in the concentration ranges of 0.6–63.5 µg/L, 2.1–207.2 µg/L, and 1.1–112.4 µg/L for Cu(II), Pb(II), and Cd(II) with a low detection limit (LOD) of 0.2 µg/L, 0.7 µg/L, and 0.4 µg/L (S/N = 3), respectively. Moreover, the mutual interference mechanism of three ions was also investigated. The sensor showed good reproducibility, stability, and anti-interference performance. Besides, the fabricated sensor detected HMIs in edible mushrooms with high recovery between 96 and 109%. This study provides a new method for the detection of HMIs in food.

Keywords Heavy metal ions · Simultaneous detection · Covalent organic framework · Interference mechanism

Highlights

1. The electrochemical sensor was developed for simultaneous detection of HMIs.
2. COF was designed and possessed abundant amino groups for effectively adsorbing HMIs.
3. CLS solved the problem of MWCNTs aggregation and cooperated with COF to detect HMIs.
4. The mutual interference mechanism between the three HMIs was analyzed and studied.

✉ Yanyan Zhang
zyyan1104@163.com

¹ School of Agricultural Engineering and Food Science, Shandong University of Technology, No.12 Zhangzhou Road, Zibo 255049, Shandong Province, China

² Shandong Provincial Engineering Research Center of Vegetable Safety and Quality Traceability, No.12 Zhangzhou Road, Zibo 255049, Shandong Province, China

³ Zibo City Key Laboratory of Agricultural Product Safety Traceability, Zibo, China

Introduction

Heavy metal contamination in the environment and food has aroused great public concern as it poses serious threat to the ecological system and humans (Doyi et al. 2018; Hu et al. 2021). So far many traditional technologies have been developed in the field of heavy metal ion (HMI) detection including laser-induced breakdown spectroscopy (LIBS), inductively coupled plasma mass spectrometry (ICP-MS), and atomic absorption spectroscopy (AAS) (Rezk et al. 2018; Xing et al. 2019; Komendova 2020). However, these technologies have some drawbacks, for instance, the high cost and large volume of the instrument make it difficult to realize rapid onsite detection of HMIs. Compared with the laboratory analysis method, electrochemical technology has become one of the main techniques for the detection of HMIs in recent years owing to the low cost, fast onsite detection, and high sensitivity (Kilele et al. 2021, 2020).

Some studies have reported that edible mushrooms can accumulate multiple HMIs in their fruit body such as copper, lead, and cadmium (Kokkoris et al. 2019; Zhang et al. 2020). However, the electrochemical detection of HMIs is currently mainly concentrated on a single heavy metal, so the design of a high sensitive approach for the simultaneous detection of multiple HMIs is of great significance for improving the efficiency of heavy metal detection. It is a challenge to achieve efficiently simultaneous detection of multiple heavy metals, because it requires not only a large number of adsorption sites on the surface of the sensor, but also a high electron transfer rate.

Certain HMIs tend to bind to ligands containing nitrogen, sulfur, and oxygen (Maciel et al. 2019; Fouda-Mbanga et al. 2021; Majdoub et al. 2021; Arduini et al. 2020; Hanif et al. 2019a; Unnikrishnan et al. 2021). One of the important factors to improve the detection efficiency of sensors is to enhance the sensitivity of sensors; nanomaterials with excellent performance can be modified on the surface of the sensor, which is beneficial to improve the performance of the sensor (Chokkareddy et al. 2020, 2021). The covalent organic framework (COF) is a newly developed porous crystal material with the characteristics of a large surface area and unique ordered channel structure (Magano et al. 2020; Bagheri et al. 2021). In addition, COF is structurally predesignated, synthetically controllable, and easy to be functionalized (Wang et al. 2020; Elwakeel et al. 2020; Skorjanc et al. 2021; Arul et al. 2020; Zhang et al. 2021). Zhang et al. (2018) prepared a COF material with a terminal unsaturated amino group in the COF as the connection by solution infiltration method; the sensor showed great electrocatalytic performance in electrochemical detection. Wang et al. (2021) prepared a novel N,S-rich COF BTT-TZT that provided abundant adsorption sites for Hg^{2+} . Hence, COF designed with a specific structure can be used for firm accumulating of HMIs. A large number of binding sites of COF provide great potential in the field of HMI detection. However, the poor electronic conductivity of COF has restricted its usability in electrochemical detection. Therefore, it is necessary to introduce highly conductive nanomaterials to improve the electrochemical performance of the sensor.

Among various nanomaterials, multiwalled carbon nanotubes (MWCNTs) are outstanding materials that not only have good electrical conductivity and high surface area but also contain many functional groups (Khan et al. 2021; Wu et al. 2020). However, MWCNTs can form insoluble large aggregates in water due to the defects and impurities in the structure, affecting the conductivity of MWCNTs (Jintoku et al. 2019). Therefore, it is necessary to introduce a dispersant to improve the stability and dispersion of MWCNTs. Calcium lignosulfonate (CLS) is an inexpensive, reproducible, and amphiphilic biopolymer with numerous hydrophilic groups, i.e., oxygen-containing groups and sulfonic groups.

CLS not only effectively solves the problem of aggregation of MWCNTs but also benefits to the adsorption of HMIs by taking the advantages of these functional groups in the structure (Sajjadi et al. 2021; Söğüt et al. 2020). Nafion is a perfluorosulfonate-polytetrafluoroethylene copolymer; it has been widely used as a modified electrode material owing to its good membrane forming ability and cation permeability (Olejnik et al. 2020; Mynttinen et al. 2020; Kumar et al. 2021). Compared with the traditional sensor based on COF, the sensor constructed in this work not only has higher adsorption performance, but also improves the poor conductivity of COF in the process of electrochemical detection, and improves the mechanical strength of the sensor. The negatively charged functional groups of COF, MWCNTs/CLS, and Nafion played a synergistic role in HMI accumulation by electrostatic interaction.

In this study, a COF/MWCNTs/CLS/Nafion/glass carbon electrode (GCE) was developed for the effective detection of HMIs. The morphological and structural analyses of COF were conducted using different characterization methods. The electrochemical characteristics based on different materials were studied by cyclic voltammetry (CV) and electrochemical impedance spectroscopy (EIS). The performance of the prepared sensor in detecting trace Cu(II), Pb(II), and Cd(II) ions was detected by SWASV (square wave anodic stripping voltammetry) under optimized experimental conditions in edible mushrooms. At the same time, the mutual interference mechanism between the target ions was analyzed to verify the scientificity of the synchronous detection of multiple HMIs in the same system. Furthermore, the reproducibility, stability, and anti-interference ability of the fabricated sensor were studied.

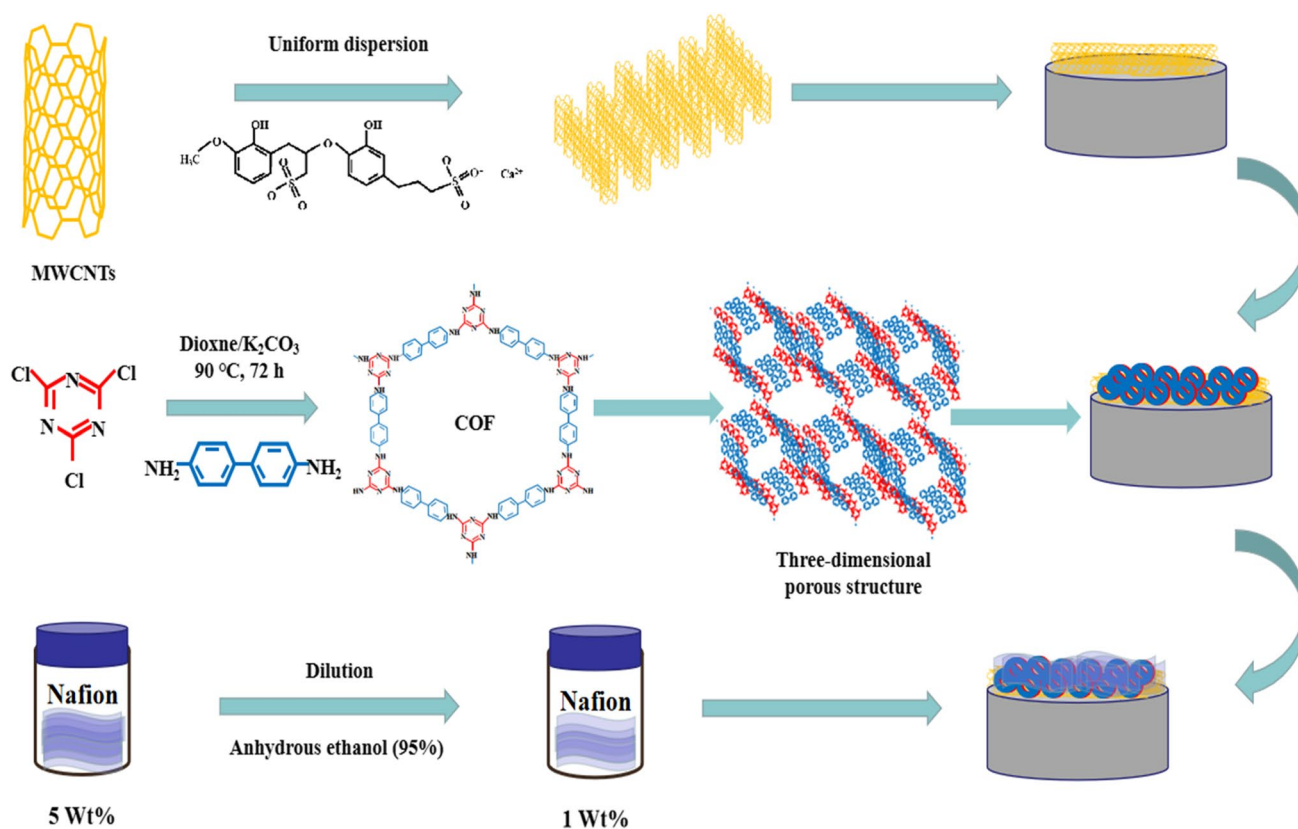
Experiments

Materials and Instruments

Nafion solution (5%) was provided by DuPont Company. MWCNTs, CLS, potassium carbonate, cyanuric chloride, and other chemicals were provided by Macklin (Shanghai, China). The standard solution of copper, lead, and cadmium were purchased from the National Pharmaceutical Reagent Company (Shanghai, China). All the reagents were analytically pure. Ultrapure water (18.2 M Ω .cm) was used in all the experiments.

Apparatus

The apparatus of this work was listed in [supplementary materials](#).



Scheme 1 Fabrication process of COF/MWCNTs/CLS/Nafion/GCE

Preparation of COF Nanocomposite

The COF nanocomposite was synthesized using a solvothermal method. First, 4 mM of melamine was slowly added to a dioxane solution (20 mL). After 30 min of ultrasound, the dioxane solution containing 6 mM of *p*-diphenylamine and 12 mM of potassium carbonate were heated on an oil bath at 90 °C for 72 h. Then, the obtained material was extracted using dichloromethane for 72 h. Finally, a solid was obtained through filtration and separation.

Preparation of MWCNTs/CLS

Briefly, MWCNTs (30 mg) were dispersed in 30-mL ultrapure water; then, the CLS (0.01 mg/mL) was added and ultrasonicated for 30 min. Finally, the mixture was rotated under vibration for 12 h and stored at 4 °C for further use.

Fabrication of COF/MWCNTs/CLS/Nafion/GCE

As shown in Scheme 1, the GCE (3 mm in diameter) was first polished using alumina powder (0.30 and 0.05 μm) before modification. Next, the GCE was used for ultrasonic in alcohol and water to thoroughly remove the residual

powder. Then, all the reagents were uniformly dispersed by ultrasonic oscillations before usage. Subsequently, 8 μL of MWCNTs/CLS, COF, and Nafion (1 wt%) solution were dripped onto the prepared bare GCE and dried under room temperature conditions in sequence. Finally, the COF/MWCNTs/CLS/Nafion/GCE nanocomposite was obtained.

Edible Mushroom Sample Preparation

The method of sample preparation was listed in [supplementary materials](#).

Results and Discussion

Characterization of COF Nanocomposite

The morphology of COF nanocomposite was studied by SEM, TEM, and EDS. As shown in Fig. 1A, the SEM images showed the overall morphology of COF with a porous structure in the image which clearly showed the dimensional structure of COF nanocomposite. The three-dimensional microstructure was shown in Fig. 1B and C; COF presented a uniform porous morphology, thus showing a large specific

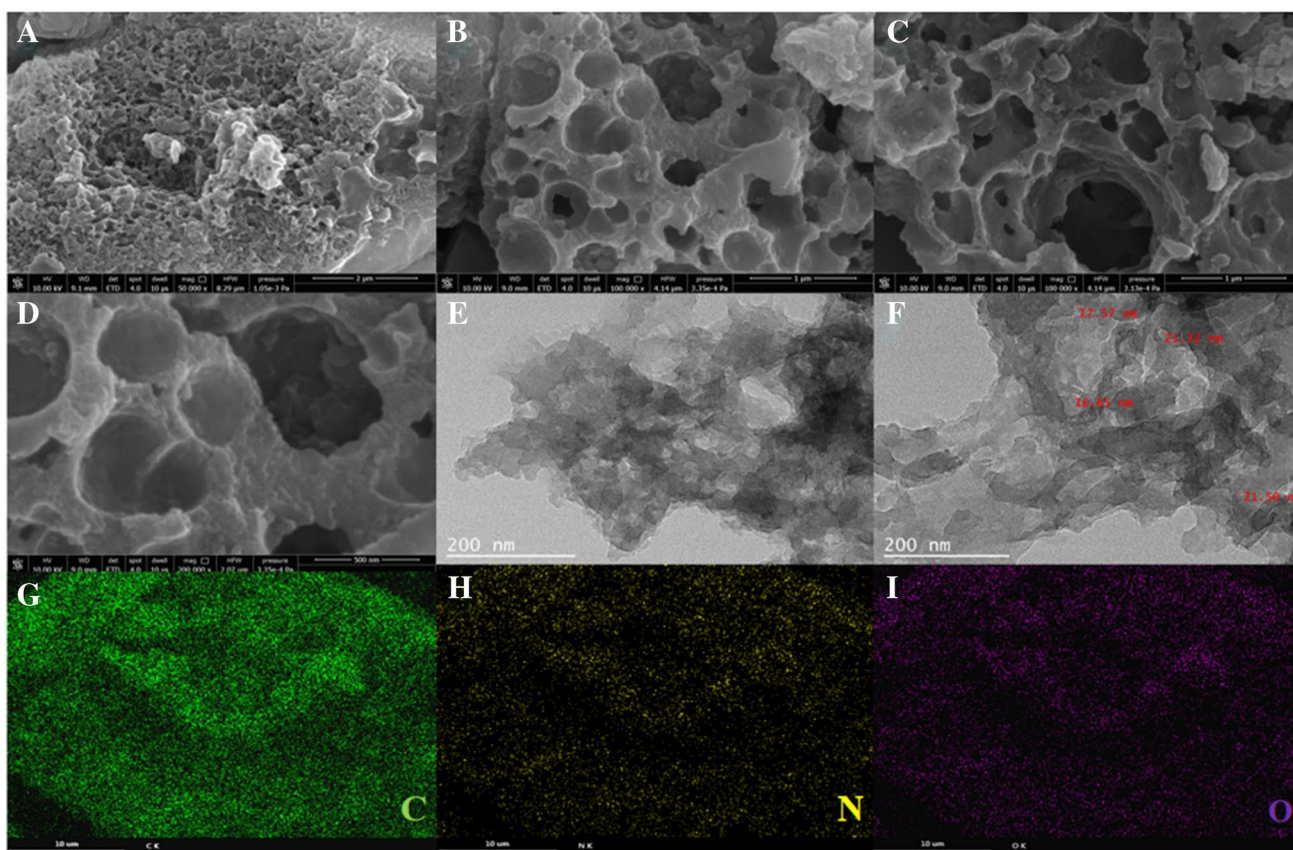


Fig. 1 A, B, C, and D SEM images of COF material; E and F TEM images of COF material; G, H, and I EDS patterns of COF material

surface area. The abundant pore structure tremendously made more heavy metal ions load onto the sensing interface, which was beneficial to improve the detection efficiency of the sensor. The advantages of COF/MWCNTs/CLS/Nafion/GCE in electrochemical detection of heavy metals were greatly enhanced. The elements of COF were analyzed by EDS. Figure 1G, H, and I shows that the C, N, and O elements were uniformly distributed on the nanocomposite. As shown in Fig. 1E and F, the TEM image further showed that the pore structure existed in COF, and the nanometer diameter was approximately around 10 nm to 20 nm. These results indicated the successful synthesis of COF.

The formation of COF nanocomposite was studied by XPS. The characteristic peaks at 532.1 eV, 400.3 eV, and 285.0 eV in the spectrum of COF correspond to the elements O, N, and C in the composite (Fig. 2A). The peaks at 399.7 and 398.7 eV in the N1s spectrum could be attributed to the pyridinic N and pyrrolic N in the COF, respectively (Fig. 2B) (Sun et al. 2016a). As shown in Fig. 3A, the FT-IR spectrum showed the C=N stretching vibrations at 1619 cm^{-1} ; the vibration bands observed at 1702 and 3316 cm^{-1} appeared were because of the N–H stretching vibrations indicating the successful synthesis of COF material (Cui et al. 2021).

Electrochemical Responses

The electrochemical characterization of different materials were studied by CV, EIS, and SWASV. CV and EIS analyses were conducted in a $5\text{ mM } [\text{Fe}(\text{CN})_6]^{3-/4-}$ solution containing 1 M KCl . As shown in Fig. 3B, the CV image of different materials indicates that the MWCNTs/CLS/GCE nanocomposite had the best electron transfer rate compared to COF/GCE, MWCNTs/GCE, Nafion/GCE, and MWCNTs/CLS, enhancing the electrical activity of COF/MWCNTs/CLS/Nafion modified sensor. The effective electroactive area is a crucial part of assessing electrochemical behavior. The effective electroactive area was determined based on the Randles–Sevcik equation.

$$I_p = 2.69 \times 10^5 AD^{1/2} n^3/2 \gamma^{1/2} C$$

In the above equation, A represents effective active surface area of the modified electrode (cm^2); D means the diffusion coefficient in solution, approximately $6.70 \times 10^{-6}\text{ cm}^2\text{ s}^{-1}$; n means the amount of electron transferred in the reaction, approximately 1; γ represents the scan rate, $0.05\text{ (V s}^{-1}\text{)}$; C represents the concentration of detected molecule (5 mM); I_p is the current of redox peak. The effective active area of

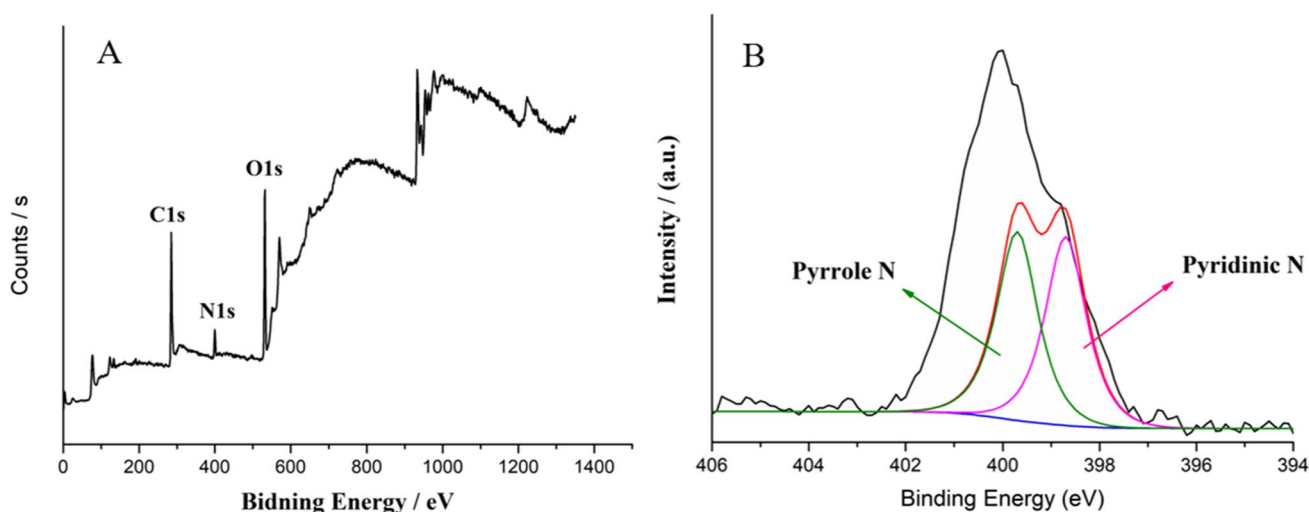


Fig. 2 A XPS full research of COF; N1s region **B** in the XPS of COF composite

COF/MWCNTs/CLS/Nafion/GCE nanocomposite for 5 mM $[\text{Fe}(\text{CN})_6]^{3-/4-}$ was 1.8 times higher than COF/GCE and 1.2 times than bare GCE as obtained through calculation; the effective active area of MWCNTs/CLS/GCE nanocomposite for 5 mM $[\text{Fe}(\text{CN})_6]^{3-/4-}$ was 1.16 times higher than MWCNTs/GCE as obtained through calculation. These results showed that MWCNTs/CLS significantly improved the conductivity of the electrode.

EIS were carried out to study the surface properties in the above electrodes. The Nyquist plots reflected the charge transfer resistance corresponding to the semicircular arc (Fig. 3C) (Motia et al. 2020). The Nafion/GCE and COF/GCE showed an enlarged semicircular arc compared to COF/MWCNTs/CLS/Nafion/GCE, indicating that the MWCNTs/CLS modified electrode significantly decreased the charge transfer resistance. However, for the MWCNTs/CLS/GCE nanocomposite, the diameters of the semicircular arc decreased compared to MWCNTs/GCE owing to the good diffusion effect of CLS. The obtained results of EIS were in accord with CV and proved that the MWCNTs/CLS nanocomposite played a positive role in improving the conductivity of the modified electrode.

As shown in Fig. 3D, the SWASV responses of different materials were tested in a HAc-NaAc buffer solution (ABS, 0.1 M, pH 5.0) containing three target ions (500 nM). A comparison of different materials indicated that the COF/MWCNTs/CLS/Nafion/GCE nanocomposite exhibited the best catalytic performance towards the detection of HMIs. The peak currents of COF/GCE, MWCNTs/CLS/GCE, and Nafion were significantly larger than the bare electrode, which could be explained in terms of abundant functional groups, electrocatalytic ability, and adsorption performance of COF, MWCNTs/CLS, and Nafion composite. The COF/MWCNTs/CLS/Nafion/GCE nanocomposite showed the largest peak current in Fig. 3D; a significant enhancement in

the electrochemical response signal can be attributed to the synergistic interaction between COF, MWCNTs, and Nafion. The number of active sites increased owing to the modification of COF and MWCNTs/CLS and the efficiency of electrochemical detection of HMIs was effectively improved.

Optimization of Experimental Conditions

To achieve the best condition for detecting HMIs based on the COF/MWCNTs/CLS/Nafion/GCE nanocomposite, the type of buffer solution, deposition time, and pH of buffer solution were optimized using the SWASV method.

The type of buffer solution significantly affected the electrochemical behavior of sensors. The effect of three different buffer solutions including phosphate buffer solution (PBS, 0.1 M, pH 5.0), ABS (0.1 M, pH 5.0), and sodium chloride buffer solution (NaCl, 0.1 M, pH 5.0) on the peak current was studied (Fig. 4A). As shown in Fig. 4A, the peak values of HMIs in the PBS and NaCl were entirely lower than the peak current in ABS. Especially, the response curves of Pb(II) and Cd(II) were inconspicuous in the NaCl solution. In comparison, it was found that the largest response curves of HMIs were well separated, and the intensities of peak currents were remarkably improved in ABS. The above results probably due to the difference in the degree of complexation between HMIs and the electrolyte solution (Hanif et al. 2019b). According to the results, ABS was selected as the electrolyte solution.

The pH values affected the peak current for the detection of HMIs (Fig. 4B). The response signals of HMIs gradually improved with the increase in pH from 3.0 to 5.0. The largest peak currents of three HMIs appeared at pH 5.0. When the pH was further increased from 5.0 to 6.0, the peak curves of three HMIs decreased on the contrary. At a comparatively low pH, the hydrophilic groups were protonated, thus weakening the absorption

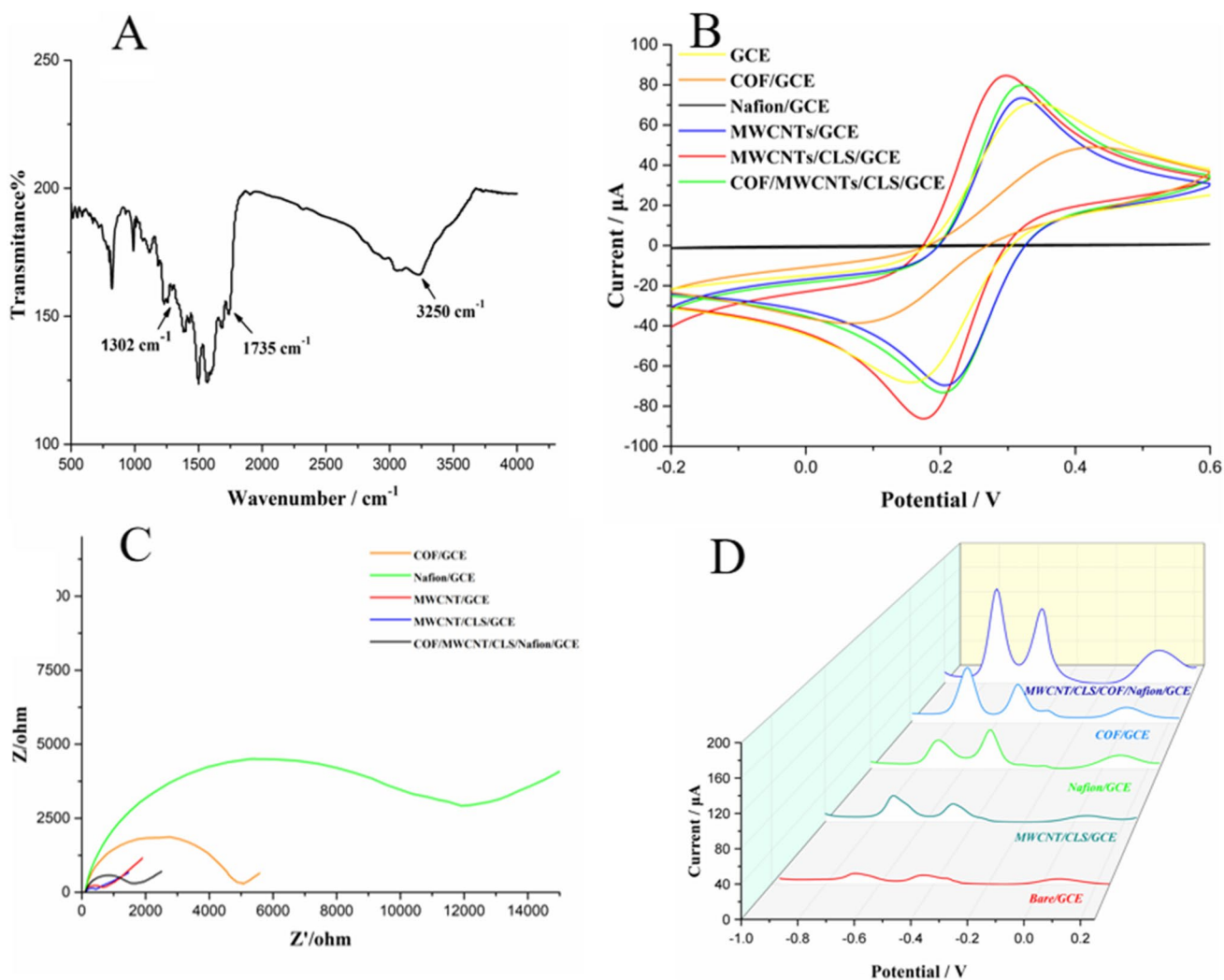


Fig. 3 **A** FT-IR spectra of the COF material; **B** CV and **C** Nyquist plots of COF/GCE, Nafion/GCE, MWCNTs/GCE, MWCNTs/CLS/GCE, and COF/MWCNTs/CLS/Nafion/GCE detected in 0.1 M KCl containing 5.0 mM $[\text{Fe}(\text{CN})_6]^{3-/4-}$; **D** SWASV curves of bare GCE,

COF/GCE, Nafion/GCE, MWCNTs/GCE, MWCNTs/CLS/GCE, and COF/MWCNT/CLS/Nafion/GCE recorded in HAc-NaAc buffer solution (pH 5.0) containing 500 nM of Cu(II), Pb(II), and Cd(II) after 480 s of accumulation at potential of -1.3 V

ability of the HMIs on the electrode materials (Hanif et al. 2019c). When the pH value was higher than pH 5.0, the reduction in the stripping peaks at high pH value exhibited a lower current value owing to the precipitation of metal ions in the form of metal hydroxide complexes which considerably decreased the existing number of metal ions in the solution. Based on these results, pH 5.0 was selected as the best pH for this study.

The dependence of stripping peaks response on the deposition time was examined in the range of 60–540 s and obtained results were shown in Fig. 4C. With the increase in deposition time, the peak current reached the maximum value at 480 s. Nevertheless, the response signals of Pb(II) and Cd(II) decreased at 500 s; the response signal of Cu(II) decreased at 510 s. This was probably because the active sites on the electrode surface tend to be saturated due to the accumulation of a great number of

HMIs (Akhtar et al. 2020). On the other hand, this phenomenon probably occurred due to the competitive adsorption of three target HMIs. Thus, some HMIs could not dissolve from the pores during the dissolution. On the basis of these results, 480 s was preferred as the ideal deposition time for further studies.

Deposition potential is a crucial parameter to obtain the best response in the electrochemical detection of HMIs. In this experiment, the effect of deposition potential towards HMIs was studied (Fig. 4D). The results show that the response signals for HMIs gradually increased with the decrease in potentials from -1.0 to -1.3 V, and the peak current for HMIs exhibited a maximum value at a potential of -1.3 V. Then, the current decreased when a more negative deposition potential was applied. Based on these results, -1.3 V was the optimum deposition potential in this study.

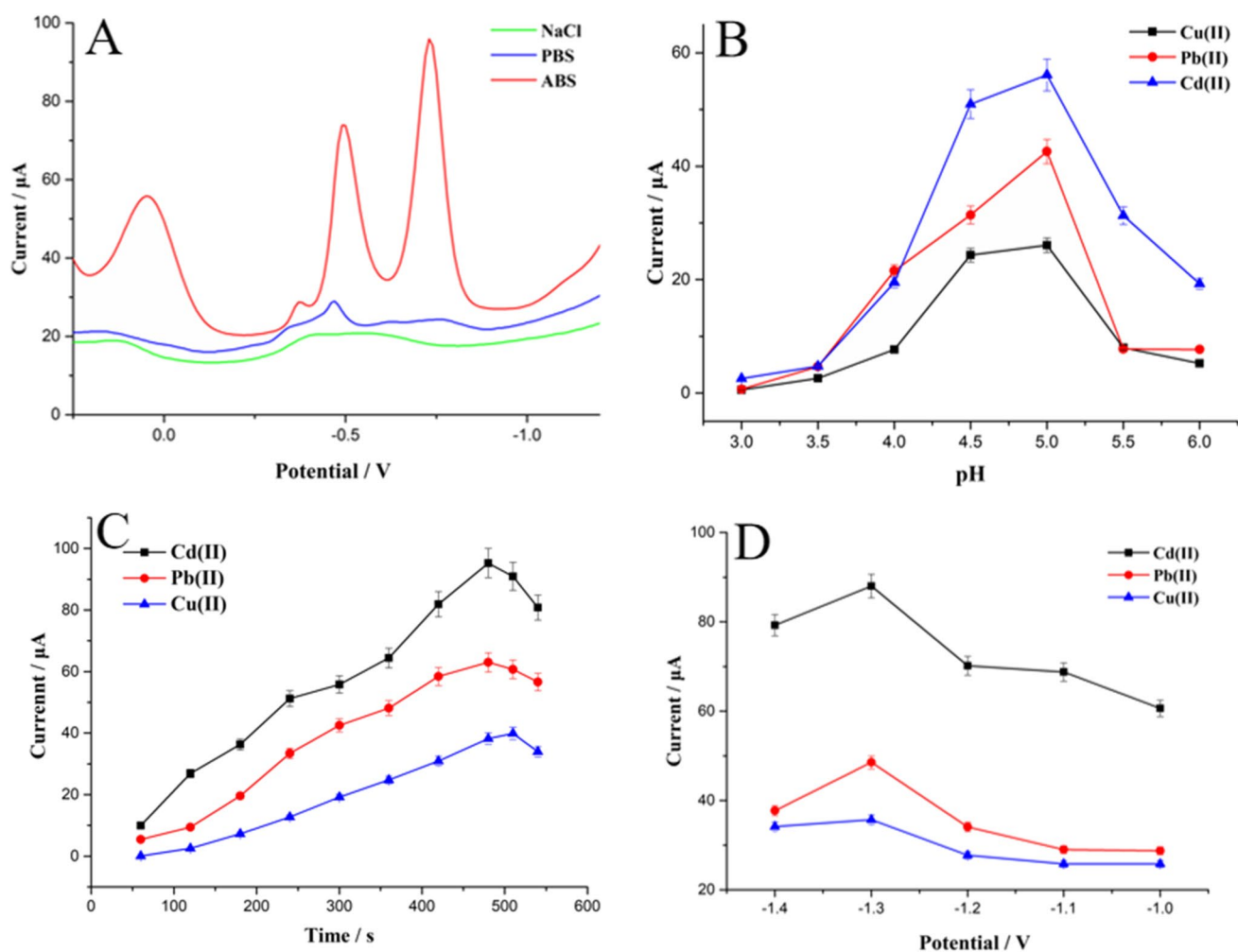


Fig. 4 Optimum experimental conditions. **A** Effect of different buffer solutions; **B** pH of detection solution (pH: 3.0–6.0); **C** accumulation time (60 s–540 s); **D** accumulation potential (–1.0––1.3 V) on the stripping peak current of Cu(II), Pb(II), and Cd(II) ions (error bar: $n = 3$)

Electrochemistry Detection of Cu(II), Pb(II), and Cd(II) Ions

Under the optimal conditions, SWASV was applied for the determination of three target ions based on COF/MWCNTs/CLS/Nafion/GCE nanocomposite in the ranges of 0.6–63.5 μg/L, 2.1–207.2 μg/L, and 1.1–112.4 μg/L for Cu(II), Pb(II), and Cd(II) ions, respectively (Fig. 5A). The linear regression equations of these three HMIs were as follows: I (μA) = 0.72C + 8.2 (μg/L) ($R^2 = 0.991$), I (μA) = 0.41C + 6.4 (μg/L) ($R^2 = 0.990$), and I (μA) = 0.48C + 46.57 (μg/L) ($R^2 = 0.991$). The limits of detection ($S/N = 3$) were calculated to be 0.2 μg/L, 0.7 μg/L, and 0.4 μg/L, respectively. The detection results of COF/MWCNTs/CLS/Nafion/GCE nanocomposite compared with other developed sensor for the electrochemical detection of the above HMIs were shown in Table 1. The fabricated sensor exhibited a wide linear response and low limit of detection, well below most reports in Table 1.

Real Edible Mushroom Sample Detection

To evaluate the practical feasibility of COF/MWCNTs/CLS/Nafion/GCE nanocomposite, the prepared sensor was tested using three different edible mushroom samples via the standard addition method. The analytical results and recoveries of the modified sensor and ICP-OES were shown in Table 2. The recoveries were in the range of 95–109%, and the detection results were close to those of ICP-OES, indicating that the COF/MWCNTs/CLS/Nafion/GCE nanocomposite could be reliably used for detecting Cu(II), Pb(II), and Cd(II) ions in actual samples.

Interference Mechanism of Coexisting Ions, Reproducibility, Stability, Anti-interference Ability

Figure 6A and B showed the interference of Pb(II) on the SWASV response of coexisting Cu(II) ions (0.1 μM) and Cd(II) ions (0.1 μM) with varying Pb(II) ion concentrations

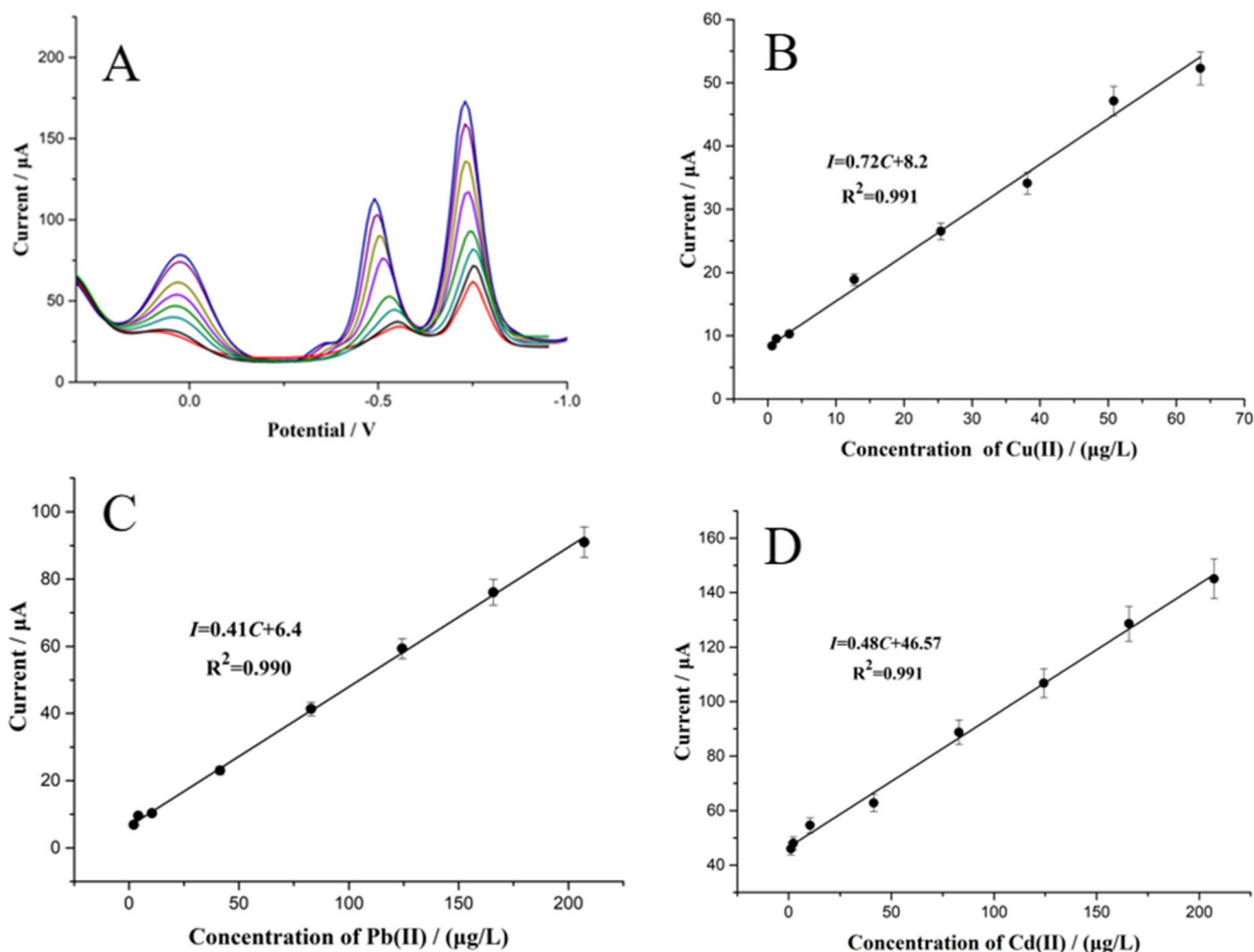


Fig. 5 A SWASV response of COF/MWCNTs/CLS/Nafion/GCE with different concentrations of Cu(II), Pb(II), and Cd(II) ions recorded in HAc-NaAc buffer solution (pH 5.0) containing 500 nM of Cu(II), Pb(II) and Cd(II) after 480 s of accumulation at potential of -1.3 V; **B, C, and D** Calibration curves of sensing platform. (Error bar: $n = 3$)

Table 1 Comparison of analytical parameters obtained using COF/MWCNTs/CLS/Nafion/GCE for Cu(II), Pb(II), and Cd(II) ion sensing with those of previous reports

Interface material	Technique	Detection range (μg L ⁻¹)			LOD (μg L ⁻¹)			Ref
		Cu(II)	Pb(II)	Cd(II)	Cu(II)	Pb(II)	Cd(II)	
AuNPs/carbon nanoflowers/GCE	SWASV	6.35–207	6.35–207	6.35–207	6.35	6.35	6.35	Zhang et al. 2016)
NH ₂ -amino-functionalized carbon microspheres	SWASV	2.54–249	2.54–249	2.54–249	0.7	11.19	6.29	Sun et al. 2016b)
graphene/polyaniline/polystyrene nano-porous fibers	SWASV	-	10–500	10–500	-	3.30	4.43	Promphet et al. 2015)
L-cysteine-RGO	DPASV	12.7–63.5	41.4–248.6	22.48–179.9	2.61	4.17	3.66	Muralikrishna et al. 2014)
GO	SWASV	6.4–95.3	20.72–310.8	11.2–168.6	3.81	5.39	6.07	Ruengpirasiri et al. 2017)
COF/MWCNTs/CLS/Nafion	SWASV	0.6–63.5	2.1–207.2	1.1–112.4	0.2	0.7	0.4	This work

(0.1–0.4 μM). No significant change in the peak current of Cd(II) was observed; the response current of Cd(II) slightly decreased with the increase in the content of Pb(II) ions.

This tendency may be caused by the competitive capture of Pb(II) and Cd(II) ions in the sensing interference (Zhu et al. 2017). Cu(II) ions were affected by Pb(II) ions owing to the

Table 2 Comparison results of Cu(II), Pb(II), and Cd(II) ions in three different mushroom samples

Sample	Original ($\mu\text{g/L}$)	Added ($\mu\text{g/L}$)			Founded ($\mu\text{g/L}$)			Recovery (%)			ICP-OES ($\mu\text{g/L}$)		
		Cu(II)	Pb(II)	Cd(II)	Cu(II)	Pb(II)	Cd(II)	Cu(II)	Pb(II)	Cd(II)	Cu(II)	Pb(II)	Cd(II)
HMIs	0												
Oyster mushroom	ND	50.8	132.5	89.9	50.6	130.0	85.4	98.9	98.1	95.0	46	133	101
Shiitake	ND	50.8	132.5	89.9	48.87	143.9	90.2	96.1	108.6	100.3	48	136	90
Hypsizygus marmoreus	ND	50.8	132.5	89.9	49.44	138.0	92.9	97.3	104.4	103.3	49	131	85

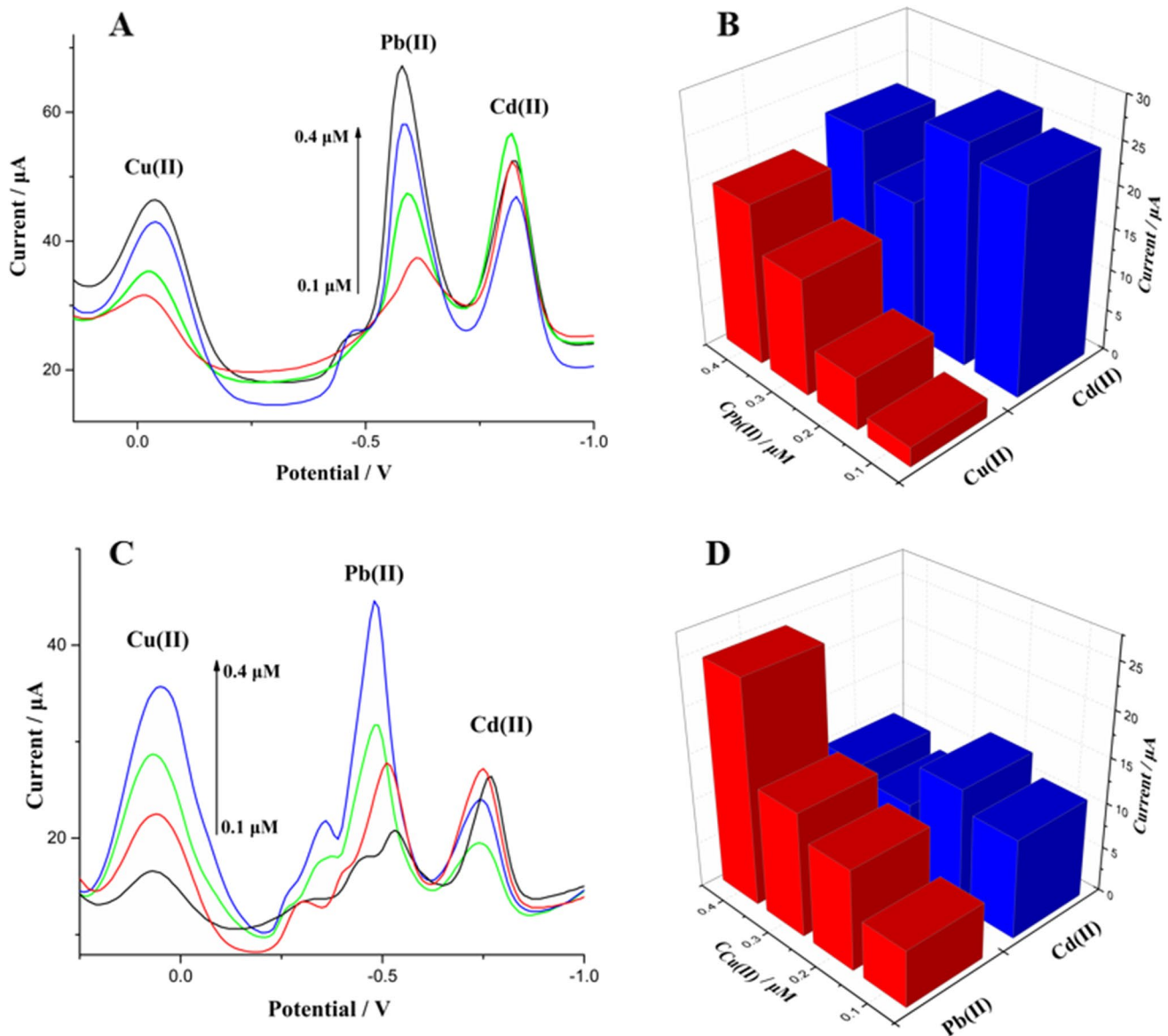


Fig. 6 **A** SWASV images of Cu(II) and Cd(II) (0.1 μM) with Pb(II) (0.2–0.4 μM); **B** peak current of coexisting ions corresponding to **A**; **C** SWASV images of Pb(II) (0.1 μM) and Cd(II) (0.1 μM) with Cu(II) (0.1–0.4 μM) by COF/MWCNTs/CLS/Nafion/GCE recorded in HAC-

NaAc buffer solution (pH 5.0) after 480 s of accumulation at potential of -1.3 V; Peak current of coexisting ions corresponding to **C**. (Error bar: $n=3$)

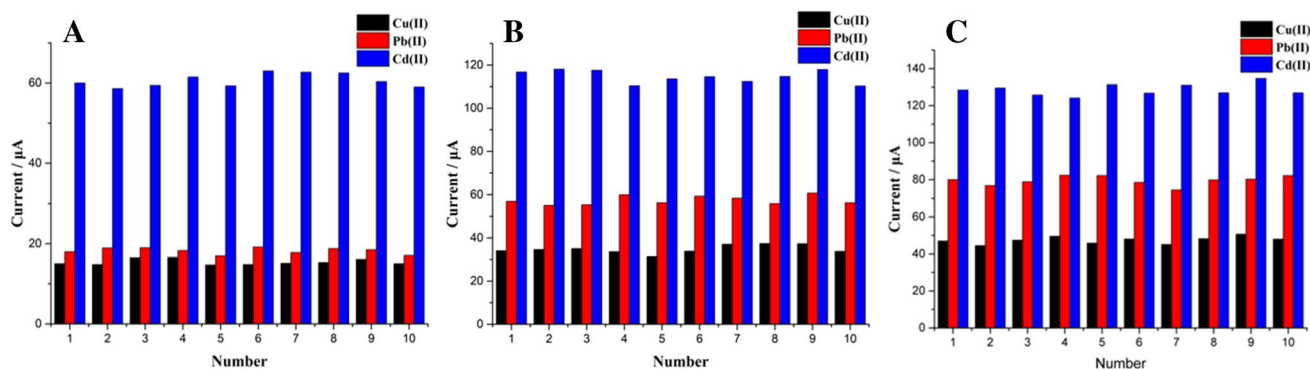


Fig. 7 **A** and **B** Reproducibility and stability assessment of the modified sensor; **C** anti-interference ability of sensor in the presence of 5 μM Mg(II), Zn(II), Ca(II), Fe(III), Ni(II), Ag(I) and mixture ion s

recorded in HAC-NaAc buffer solution (pH 5.0) containing 500 nM of Cu(II), Pb(II) and Cd(II) after 480 s of accumulation at potential of -1.3 V

formation of an intermetallic compound on the surface of the electrode; thus, the sensitivity toward Cu(II) ions improved with the increase in the content of Pb(II) ions (Durai and Badhulik 2020). The interference of Cu(II) (0.1–0.4 μM) towards Pb(II) ions (0.1 μM) and Cd(II) ions (0.1 μM) was shown in Fig. 6C and D. Similarly, slight changes in the peak current ranges were recorded for Cd(II) ions with the increase in the concentration of Cu(II) ions. However, the response signal of Pb(II) clearly increased with the concentration. This was probably because of the formation of a Cu film, followed by the formation of Cu-Pb intermetallic compounds in the process of simultaneous accumulation.

A total of 30 electrodes were prepared from the same batch and evaluated the reproducibility of the sensor by detecting of three concentrations of Cu(II), Pb(II), and Cd(II). Figure 7(A), (B), and (C) showed the reproducibility of the sensor under

the conditions of different concentrations of heavy metal ions. The RSDs derived from the ten currents for three HMIs were 4.72%, 4.03%, and 3.01% at concentration of 200 nM; when the concentration of three HMIs was 600 nM, the RSDs are 5.56%, 3.44%, and 2.59%, and the RSDs of three HMIs were 4.34%, 3.02% and 3.29% at concentration of 800 μM . These results indicated that COF/MWCNTs/CLS/Nafion modified electrode exhibited excellent reproducibility for repeated electrochemical determination of HMIs.

Furthermore, the long-term stability of COF/MWCNTs/CLS/Nafion/GCE nanocomposite was also studied (Fig. 8A). The high stability of the sensor was verified by testing the numerical change of peak current within 30 days. The test was conducted every 5 days, and the results showed that the fabricated sensors exhibit excellent stability for four weeks with an initial current response of 94.2%.

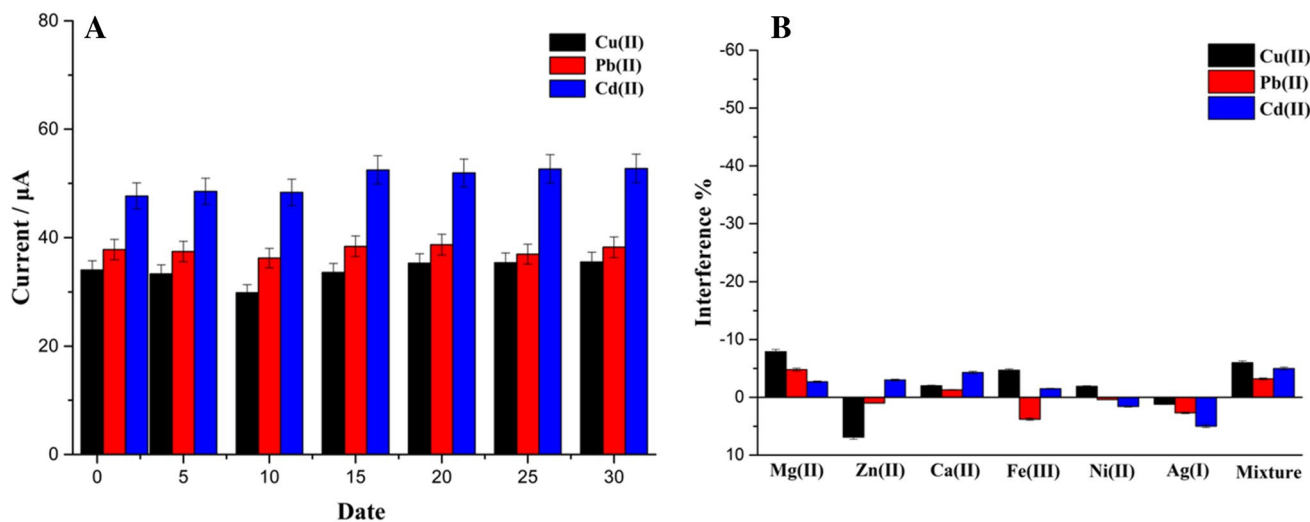


Fig. 8 **A** Stability within 30 days under room temperature and **B** anti-interference ability of sensor in the presence of 5 μM Mg(II), Zn(II), Ca(II), Fe(III), Ni(II), Ag(I), and mixture ions recorded in HAC-NaAc

buffer solution (pH 5.0) containing 500 nM of Cu(II), Pb(II), and Cd(II) after 480 s of accumulation at potential of -1.3 V. (Error bar: $n=3$)

In order to evaluate the anti-interference ability of the current sensing system, the effects of other cations at a concentration of 10 times that of target ions were evaluated by SWASV. Figure 8B showed that the response current changed slightly after adding interference metal ions and mixture interference ions in actual edible mushroom samples. The results indicated that this new strategy had good selectivity for HMI determination. Therefore, the sensing performance of COF/MWCNTs/CLS/Nafion/GCE nanocomposite is expected to be acceptable for the detection of these three HMIs in actual edible mushroom samples.

Conclusion

This work demonstrates an efficient electrochemical sensor based on 3D porous COF, MWCNTs/CLS, and Nafion with excellent electrochemical characteristics. COF materials were synthesized by simple hydrothermal method, and the morphology and composition of the materials were studied by various characterization methods. The successful synthesis of the material was proved by various characterization methods. The COF/MWCNTs/CLS/Nafion/GCE nanocomposite had a unique surface structure, high adsorption efficiency, and numerous active sites such as amino, sulfonic group, and carboxyl groups, which could improve the complexation ability of HMIs. The influence of the type of buffer solution, deposition time, deposition point, and pH value on the electrochemical detection of heavy metals was studied. In addition, COF/MWCNTs/CLS/Nafion/GCE exhibited excellent stability, reproducibility, as well as anti-interference ability towards detection of Cu(II), Pb(II), and Cd(II) with LOD of 0.2 µg/L, 0.7 µg/L, and 0.4 µg/L, respectively. The sensor was applied to the detection of edible mushroom samples; the recoveries were in the range of 95–109%. This study provides a new strategy for material synthesis and application to the electrochemical analysis of HMIs, which is expected to monitor food safety in the planting source.

Supplementary Information The online version contains supplementary material available at <https://doi.org/10.1007/s12161-022-02369-1>.

Author Contribution Jiaqi Yin (conceptualization, investigation, writing—original draft, formal analysis, methodology, validation)

Hongguo Zhai (investigation, formal analysis, writing—review and editing)

Yue Wang (formal analysis, visualization, software, supervision)

Bao Wang (formal analysis, software, supervision)

Guanglei Chu (formal analysis, supervision)

Qi Go (formal analysis, visualization)

Yuhao Zhang (visualization, software, supervision)

Xia Sun (supervision, project administration)

Yemin Guo (supervision, resources)

Yanyan Zhang (project administration, writing—review and editing, funding acquisition, resources)

Funding This work was supported by the Shandong natural science foundation-PhD foundation (ZR2018BC055), research on mechanism and analysis method of biosensor based heavy metal synchronization detection in agricultural products.

Data Availability Statement The datasets generated during and/or analyzed during the current study are available from the corresponding author on reasonable request.

Declarations

Conflict of Interest The authors declare no competing interests.

References

- Akhtar M, Tahir A, Zulfiqar S, Hanif F, Warsi MF, Agboola PO, Shakir I (2020) Ternary hybrid of polyaniline-alanine-reduced graphene oxide for electrochemical sensing of heavy metal ions. *Synth Met* 265:116410
- Arduini F, Cintic S, Mazzaracchio V, Scognamiglio V, Amine A, Moscone D (2020) Carbon black as an outstanding and affordable nanomaterial for electrochemical (bio)sensor design. *Biosens Bioelectron* 156:112033
- Arul P, Narayanamoorthi E, John SA (2020) Covalent organic framework film as an effective electrocatalyst for the simultaneous determination of dihydroxybenzene isomers in water samples. *Sensors Actuators B Chem* 313:128033
- Bagheri AR, Aramesh N, Sher F, Bilal M (2021) Covalent organic frameworks as robust materials for mitigation of environmental pollutants. *Chemosphere* 270:129523
- Chokkareddy R, Kanchi S, Inamuddin (2020) Simultaneous detection of ethambutol and pyrazinamide with IL@CoFe₂O₄NPs@MWCNTs fabricated glassy carbon electrode. *Sci Rep* 10:1
- Chokkareddy R, Thondavada N, Kabane B, Redhi GG (2021) A novel ionic liquid based electrochemical sensor for detection of pyrazinamide. *J Iran Chem Soc* 18:621–629
- Cui J, Kan L, Li Z, Yang L, Wang M, He L, Lou Y, Xue Y, Zhang Z (2021) Porphyrin-based covalent organic framework as bioplatform for detection of vascular endothelial growth factor 165 through fluorescence resonance energy transfer. *Talanta* 228:122060
- Doyi I, Essumang D, Gbeddy G, Dampare S, Kumassah E, Saka D (2018) Spatial distribution, accumulation and human health risk assessment of heavy metals in soil and groundwater of the Tano Basin, Ghana. *Ecotoxicol Environ Saf* 165:540–546
- Durai L, Badhulik S (2020) Simultaneous sensing of copper, lead, cadmium and mercury traces in human blood serum using orthorhombic phase aluminium ferrite. *Mater Sci Eng C* 112:110865
- Elwakeel KZ, Shahat A, Khan ZA, Alshitari W, Guibal E (2020) Magnetic metal oxide-organic framework material for ultrasonic-assisted sorption of titan yellow and rose bengal from aqueous solutions. *Chem Eng J* 392:123635
- Fouda-Mbanga BG, Prabakaran E, Pillay K (2021) Carbohydrate biopolymers, lignin based adsorbents for removal of heavy metals (Cd²⁺, Pb²⁺, Zn²⁺) from wastewater, regeneration and reuse for spent adsorbents including latent fingerprint detection: A review. *Biotechnol Rep* 30:e00609
- Hanif F, Tahir A, Akhtar M, Waseem M, Haider S, Aly Aboud MF, Shakir I, Imran M, Warsi MF (2019a) Ultra-selective detection of Cd²⁺ and Pb²⁺ using glycine functionalized reduced graphene oxide/polyaniline nanocomposite electrode. *Synth Met* 257:116185

- Hanif F, Tahir A, Akhtar M, Waseem M, Haider S, Aboud MFA, Shakir I, Imran M, Warsi MF (2019b) Ultra-selective detection of Cd²⁺ and Pb²⁺ using glycine functionalized reduced graphene oxide/polyaniline nanocomposite electrode. *Synth Met* 257:116185
- Hanif F, Tahir A, Akhtar M, Waseem M, Haider S, Aboud MFA, Shakir I, Imran M, Warsi MF (2019c) Ultra-selective detection of Cd²⁺ and Pb²⁺ using glycine functionalized reduced graphene oxide/polyaniline nanocomposite electrode. *Synth Met* 257:116185
- Hu J, Li Z, Zhai C, Zeng L, Zhu M (2021) Photo-assisted simultaneous electrochemical detection of multiple heavy metal ions with a metal-free carbon black anchored graphitic carbon nitride sensor. *Anal Chim Acta* 1183:338951
- Jintoku H, Matsuzawa Y, Yoshida M (2019) Dual use of anionic azobenzene derivative as dispersant and dopant for carbon nanotubes for enhanced thermal stability of transparent conductive films. *Carbon* 152:247–254
- Khan FSA, Mubarak NM, Tan YH, Khalid M, Karri RR, Walvekar R, Abdullah EC, Nizamuddin S, Mazari SA (2021) A comprehensive review on magnetic carbon nanotubes and carbon nanotube-based buckypaper for removal of heavy metals and dyes. *J Hazard Mater* 413:125375
- Kilele JC, Chokkareddy R, Rono N, Redhi GG (2020) A novel electrochemical sensor for selective determination of theophylline in pharmaceutical formulations. *J Taiwan Inst Chem Eng* 111:228–238
- Kilele JC, Chokkareddy R, Redhi GG (2021) Ultra-sensitive electrochemical sensor for fenitrothion pesticide residues in fruit samples using IL@CoFe₂O₄NPs@MWCNTs nanocomposite. *Microchem J* 164:106012
- Kokkoris V, Massas I, Polemis E, Koutrotsios G, Zervakis GI (2019) Accumulation of heavy metals by wild edible mushrooms with respect to soil substrates in the Athens metropolitan area (Greece). *Sci Total Environ* 685:280–296
- Komendova R (2020) The HR-CS-GF-AAS determination and preconcentration of palladium in contaminated urban areas, especially in lichens. *Environ Pollut* 256:113468
- Kumar S, Tripathy S, Singh OK, Singh SG (2021) Cerium oxide nanofiber based electroanalytical sensor for TNF- α detection: improved interfacial stability with Nafion. *Bioelectrochemistry* 138:107725
- Maciel JV, Durigon AMM, Souza MM, Quadrado RFN, Fajardo AR, Dias D (2019) Polysaccharides derived from natural sources applied to the development of chemically modified electrodes for environmental applications: a review. *Trends Environ Anal Chem* 22:e00062
- Magano AL, Prats AEP, Cabrera S, Ballesté RM, Alemán J (2020) Incorporation of photocatalytic Pt(II) complexes into imine-based layered covalent organic frameworks (COFs) through monomer truncation strategy. *Appl Catal B Environ* 272:119027
- Majdoub M, Amedlous A, Anfar Z, Jada A, Alem NE (2021) Engineering of amine-based binding chemistry on functionalized graphene oxide/alginate hybrids for simultaneous and efficient removal of trace heavy metals: towards drinking water. *J Colloid Interface Sci* 589:511–524
- Motia S, Bouchikhi B, Llobet E, Baria NE (2020) Synthesis and characterization of a highly sensitive and selective electrochemical sensor based on molecularly imprinted polymer with gold nanoparticles modified screen-printed electrode for glycerol determination in wastewater. *Talanta* 216:120953
- Muralikrishna S, Sureshkumar K, Varley TS, Nagaraju DH, Ramakrishnappa T (2014) In situ reduction and functionalization of graphene oxide with l-cysteine for simultaneous electrochemical determination of cadmium(II), lead(II), copper(II), and mercury(II) ions. *Anal Methods* 6:8698–8705
- Mynttinen E, Wester N, Lilius T, Kalso E, Mikladal B, Varjos I, Sainio S, Jiang H, Kauppinen EI, Koskinen J, Laurila T (2020) electrochemical detection of oxycodone and its main metabolites with Nafion-coated single-walled carbon nanotube electrodes. *Anal Chem* 12:8218–8227
- Olejnik A, Karczewski J, Dołęga A, Siuzdak K, Grochowska K (2020) Novel approach to interference analysis of glucose sensing materials coated with Nafion. *Bioelectrochemistry* 135:107575
- Promphet N, Rattananat P, Rangkupan R, Chailapakul O, Rodthongkum N (2015) An electrochemical sensor based on graphene/polyaniline/polystyrene nanoporous fibers modified electrode for simultaneous determination of lead and cadmium. *Sensors Actuators B Chem* 207:526–534
- Rezk RA, Galmed AH, Abdelkreem M, Abdel Ghany NA, Harith MA (2018) Detachment of Cu (II) and Co (II) ions from synthetic wastewater via adsorption on Lates niloticus fish bones using LIBS and XRF. *J Adv Res* 14:1–9
- Ruengpirasiri P, Punrat E, Chailapakul O, Chuanwatanakul S (2017) Graphene oxide-modified electrode coated with in-situ antimony film for the simultaneous determination of heavy metals by sequential injection-anodic stripping voltammetry. *Electroanalysis* 29:1022–1030
- Sajjadi M, Ahmadpoor F, Nasrollahzadeh M, Ghafari H (2021) Lignin-derived (nano)materials for environmental pollution remediation: current challenges and future perspectives. *Int J Biol Macromol* 178:394–423
- Skorjanc T, Shetty D, Trabolsi A (2021) Pollutant removal with organic macrocycle-based covalent organic polymers and frameworks. *Chem* 7:882–918
- Söğüt EG, Karataş Y, Gülcan M, Kılıç NÇ (2020) Enhancement of adsorption capacity of reduced graphene oxide by sulfonic acid functionalization: Malachite green and Zn (II) uptake. *Mater Chem Phys* 256:123662
- Sun T, Xu L, Li S, Chai W, Huang Y, Yan Y, Chen J (2016a) Cobalt-nitrogen-doped ordered macro-mesoporous carbon for highly efficient oxygen reduction reaction. *Appl Catal B* 193:1–8
- Sun YF, Zhao LJ, Jiang TJ, Li SS, Yang M, Huang XJ (2016b) Sensitive and selective electrochemical detection of heavy metal ions using amino-functionalized carbon microspheres. *J Electroanal Chem* 760:143–150
- Unnikrishnan B, Lien C-W, Chu HW, Huang CC (2021) A review on metal nanozyme-based sensing of heavy metal ions: challenges and future perspectives. *J Hazard Mater* 401:123397
- Wang Q, Li R, Zhao Y, Zhe T, Bu T, Sun X, Sun H, Zhang M, Zheng X, Wang L (2020) Surface morphology-controllable magnetic covalent organic frameworks: a novel electrocatalyst for simultaneously high-performance detection of p-nitrophenol and o-nitrophenol. *Talanta* 219:121255
- Wang L, Yang Y, Liang H, Wu N, Peng X, Wang L, Song Y (2021) A novel N, S-rich COF and its derived hollow N, S-doped carbon@Pd nanorods for electrochemical detection of Hg²⁺ and paracetamol. *J Hazard Mater* 409:124528
- Wu Y, Deng P, Tian Y, Ding Z, Li G, Liu J, Zuberi Z, He Q (2020) Rapid recognition and determination of tryptophan by carbon nanotubes and molecularly imprinted polymer-modified glassy carbon electrode. *Bioelectrochemistry* 131:107393
- Xing G, Sardar MR, Lin B, Lin J-M (2019) Analysis of trace metals in water samples using NOBIAS chelate resins by HPLC and ICP-MS. *Talanta* 204:50–56
- Zhang B, Chen J, Zhu H, Yang T, Zou M, Zhang M, Du M (2016) Facile and green fabrication of size-controlled AuNPs/CNFs hybrids for the highly sensitive simultaneous detection of heavy metal ions. *Electrochim Acta* 196:422–430

- Zhang T, Chen Y, Huang W, Wang Y, Hu X (2018) A novel AuNPs-doped COFs composite as electrochemical probe for chlorogenic acid detection with enhanced sensitivity and stability. *Sensors Actuators B Chem* 276:362–369
- Zhang J, Barańkiewicz D, Hanć A, Falandysz J, Wang Y (2020) Contents and health risk assessment of elements in three edible ectomycorrhizal fungi (Boletaceae) from polymetallic soils in Yunnan Province, SW China. *Biol Trace Elem Res* 195:250–259
- Zhang M, Yan X, Ma W, He Y, Cai Z, Lin Z (2021) Facile synthesis of tubular magnetic fluorinated covalent organic frameworks for efficient enrichment of ultratrace polybrominated diphenyl ethers from environmental samples. *Talanta* 221:121651
- Zhu X, Liu B, Hou H, Huang Z, Zeinu KM, Huang L et al (2017) Alkaline intercalation of Ti_3C_2 MXene for simultaneous electrochemical detection of Cd(II), Pb(II), Cu(II) and Hg(II). *Electrochim Acta* 248:46–57

Publisher's Note Springer Nature remains neutral with regard to jurisdictional claims in published maps and institutional affiliations.

Springer Nature or its licensor holds exclusive rights to this article under a publishing agreement with the author(s) or other rightsholder(s); author self-archiving of the accepted manuscript version of this article is solely governed by the terms of such publishing agreement and applicable law.